MOLECULAR MEDICINE REPORTS 13: 4705-4714, 2016

Herbal medicine Gan-fu-kang downregulates Wnt/Ca^{2+} signaling to attenuate liver fibrogenesis *in vitro* and *in vivo*

YUJIE JIA[1*], LIJUN YUAN[2*], TINGTING XU[1], HANSHU LI[1], GUANG YANG[1], MIAONA JIANG[1], CAIHUA ZHANG[1] and CONG LI[1]

[1]Department of Pathophysiology, Dalian Medical University, Dalian, Liaoning 116044; [2]Department of Hematology, PLA General Hospital, Beijing 100853, P.R. China

Received April 15, 2015; Accepted January 27, 2016

DOI: 10.3892/mmr.2016.5148

Abstract. The present study was designed to verify the effect of the Chinese prescription Gan-fu-kang (GFK) on the treatment of liver fibrosis, and to investigate its underlying mechanisms. Liver fibrosis was established in rats by the subcutaneous administration of 0.5 mg/kg carbon tetrachloride (CCl_4) twice a week for 8 weeks. Subsequently, the rats were divided into four CCl_4 groups, which were treated daily with vehicle and GFK (31.25, 312.5 and 3,125 mg/kg/day) orally between weeks 9 and 20. The inhibitory action of GFK-medicated serum on platelet-derived growth factor (PDGF)-stimulated HSC-T6 cells was also investigated. Biochemical parameters, hydroxyproline (Hyp) content and histological changes to the liver were measured. Reverse transcription-quantitative polymerase chain reaction, western blotting and immunohistochemistry were used to examine the expression of α-smooth muscle actin (α-SMA), PDGF-BB, PDGF receptor β, collagen type I and II, and the Wnt/Ca^{2+} signaling pathway. The results showed that GFK significantly alleviated the histological changes, decreased the content of Hyp in the liver and improved liver function in rats. In addition, GFK and GFK-medicated serum effectively inhibited collagen deposition, reduced the expression of α-SMA and downregulated the Wnt/Ca^{2+} signaling pathway *in vivo* and *in vitro*, respectively, as well as cell viability ($P<0.05$). These results indicated that GFK was effective in attenuating liver injury and fibrosis through downregulation of the Wnt/Ca^{2+} signaling pathway.

Correspondence to: Ms. Caihua Zhang or Ms. Cong Li, Department of Pathophysiology, Dalian Medical University, South Road West Section 9, Lvshunkou, Dalian, Liaoning 116044, P.R. China
E-mail: pathophy@hotmail.com
E-mail: goodluck_licong@163.com

[*]Contributed equally

Key words: liver fibrosis, Gan-fu-kang, hepatic stellate cells, Wnt/Ca^{2+} signaling pathway, platelet-derived growth factor

Introduction

Liver fibrosis is a common wound-healing response of the liver to a variety of chronic injuries, including infections, particularly hepatitis B or C, alcoholic steatohepatitis, non-alcoholic steatohepatitis and toxic agents, and is characterized by an excessive deposition of extracellular matrix (ECM) (1,2). It has been demonstrated that activated hepatic stellate cells (HSCs) are the predominant cell type responsible for ECM accumulation in the liver, and their activation is associated with specific cytoskeletal and phenotypic profiles (3,4). Therefore, the majority of antifibrotic therapies are designed to inhibit the activation and proliferation of HSCs. Platelet-derived growth factor (PDGF) is the most potent mitogenic and proliferative cytokine described for HSCs (5). PDGF-BB is the most potent PDGF isoform and has been shown to be the most effective stimulator of HSC proliferation (6). PDGF receptor β (PDGFRβ) amplifies biological responses to PDGF-BB, leading to the activation of downstream signaling pathways in HSCs (7).

The Wnt signaling pathway is essential for embryogenesis and adult tissue maintenance, and disturbance in this signaling promotes neurodegenerative diseases and cancer (8-10). There are two predominant Wnt signaling pathways: The canonical Wnt/β-catenin pathway and the non-canonical Wnt/Ca^{2+} pathway. In previous decades, the canonical and non-canonical Wnt signaling pathway have been reported to be important in liver development and remodeling, and HSC activation (11-13). Previously, it was reported that the Wnt/Ca^{2+} signaling pathway can be activated in human HSCs induced by PDGF-BB, and is involved in HSC activation and proliferation (14). However, the role of the non-canonical Wnt signaling pathway in this specific pathophysiological process has received little attention, and remains to be fully elucidated, particularly concerning the Wnt/Ca^{2+} signaling pathway (15).

Traditional Chinese herbs have been widely used as hepatoprotective and antifibrotic drugs in humans (16) and animal models (17), with novel characteristics, including being multi-ingredient, multi-targeting and with low adverse effects. Gan-fu-kang (GFK) is a complex prescription Chinese herbal medicine composed of 11 medical herbs, including *Salvia miltiorrhiza*, *Astragalus membranaceus*, red peony root, white peony root, Radix paeoniae alba and Chinese thorowax root (18). This herbal formula is considered to have effects in increasing blood volume, energy and blood flow to the liver (18). Our pilot study showed that GFK has markedly protective and therapeutic effects in an animal model of hepatic injury induced by carbon tetrachloride (CCl_4) (18). Mechanistic investigations have shown that GFK downregulates the mitogen-activated protein kinase/activator protein 1 pathway (19) and canonical Wnt/β-catenin signaling pathway (20) in the fibrotic liver. However, the mechanism by which GFK inhibits liver fibrosis remains to be fully elucidate.

The aim of the present study was to examine the protective effect of GFK on hepatic fibrosis in liver tissues from Sprague-Dawley rats and HSC-T6 cells. Furthermore, the present study aimed to confirm whether GFK attenuates hepatic fibrosis via the Wnt/Ca^{2+} pathway to elucidate the possible underlying mechanism of its anti-fibrotic effect.

Materials and methods

Herbal medicine composition. GFK consists of 11 herbs, including 30 g each of Salviae miltiorrhizae radix and Milkvetch root; 20 g each of Fructus aurantii and Hoelen; 15 g each of Radix paeoniae rubra, Radix paeoniae alba, Radix angelicae sinensis, Radix rehmanniae and Rhizoma atractylodis macrocephalae; and 10 g each of Radix bupleuri and Radix glycyrrhizae (Table I). The 11 crude drugs were purchased from the pharmacy of the Second Affiliated Hospital of Dalian Medical University (Dalian, China) and extracted by the Department of Pathophysiology of Dalian Medical University. The herbal decoction was stored at -20˚C.

Animals. Sprague-Dawley rats (n=53; 26 male and 27 female; weight, 180-220 g; age, 6 weeks) were supplied by the Experimental Animal Center of Dalian Medical University [confirmation no. SCXK (Liao) 2004-0017]. The rats were housed in an air-conditioned room at 22±1˚C, with 50-60% relative humidity and a 12 h light-dark cycle, and were fed a standard laboratory diet and tap water *ad libitum*. The experiments were performed in accordance with the principles and guidelines for the human treatment of animals set by the National Institutes of Health Guide (NIH publication no. 85-23, revised 1985) (21) and was approved by the ethics committee of Dalian Medical University.

Experimental model and drug treatment. The rats were randomly divided into five groups: Normal control group (n=12), CCl_4 (Tianjin Guangfu Fine Chemical Research Institute, Tianjin, China) model group (n=8) and three GFK groups (n=11). These rats were treated by subcutaneous injection of CCl_4 (0.5 mg/kg in a vehicle of olive oil; twice/week) for 8 weeks, with the exception of the rats in the normal control group, which were treated with vehicle only. In the treatment groups, the rats received GFK via oral administration (31.25, 312.5 and 3,125 mg/kg/day) between weeks 9 and 20. The model group and the normal control group were administered with an equal volume of normal saline. All rats were sacrificed by cervical dislocation under diethyl ether (Nanjing Chemical Reagent Co., Ltd., Nanjing, China) anesthesia at the end of week 20. Blood (~4 ml) and complete liver samples were obtained for further examination.

Preparation of drug-medicated serum. A total of 20 rats were randomly divided into two groups. Sera was obtained from the rats, following administration with normal saline or GFK at the middle dose (312.5 mg/kg/day) by gavage for 7 days.

Biochemical determination. The levels of alanine aminotransferase (ALT), aspartate aminotransferase (AST), albumin (ALB) and globulin in the serum samples were determined using a commercial test reagent (Nanjing Jiancheng Bioengineering Institute, Nanjing, China). ALB was determined in 0.02 ml serum using bromocresol green colorimetry and total protein (TP) was determined by Coomassie brilliant blue colorimetry in 0.05 ml serum. The samples were incubated with either reagent for 10 min at room temperature prior to measuring optical density at 628 nm (bromocresol green) or 595 nm (Coomassie brilliant blue) on a spectrophotometer (721; Shanghai Optical Instrument Factory, Shanghai, China).

Histopathological examination. The rat liver tissues were fixed in 10% formalin (Nanjing Chemical Reagent Co., Ltd.), embedded in paraffin (Sigma-Aldrich, St. Louis, MO, USA), cut (4 μm) and stained with either hematoxylin and eosin (H&E; Nanjing Jiancheng Bioengineering Institute) or with Picric Sirius red (Nanjing Jiancheng Bioengineering Institute). The sections were examined by light microscope (Eclipse 50i; Nikon Corporation, Tokyo, Japan), and the collagen type I and type III staining by Picric Sirius red were observed by polarizing microscope (CX31P; Olympus Corporation, Tokyo, Japan). The liver fibrosis was evaluated by a pathologist in a blinded-manner, and scored and graded according to the method of Scheuer (22), as follows: Stage 0, no fibrosis; stage 1, fibrosis expansion of certain portal areas; stage 2, formation of fibrous septa around the portal area; stage 3, fibrosis with architectural distortion, complete septa interconnecting with each; stage 4, early cirrhosis or cirrhosis.

Hepatic hydroxyproline (Hyp) assay. The content of Hyp was measured spectrophotometrically using a commercially available kit (Nanjing Jiancheng Bioengineering Institute). The quantities of Hyp in the rat liver are expressed as μg/g wet tissue.

Cell culture and 3-4,5-Dimethylthiazol-2-yl)-2,5-dipheny ltetrazolium bromide (MTT) assay. The rat HSC-T6 cell line was provided by Professor Lie-Ming Xu (Shanghai University of Chinese Traditional Medicine, Shanghai, China). The cells were cultured in Dulbecco's modified Eagle's medium (DMEM; Gibco; Thermo Fisher Scientific, Inc., Waltham, MA, USA) supplemented with 10% fetal bovine serum (Tianjin Haoyang Biological Manufacture Co., Ltd., Tianjin, China), 100 U/ml penicillin and 100 U/ml streptomycin (Sigma-Aldrich), and incubated at 37˚C in 5% CO_2 air. Following 2 weeks of culture on plastic tissue-culture dishes, the cells were plated at a density of $2x10^4$ cells/well in 96-well plates. In this experiment, these HSCs were randomly divided into three groups: Control group, PDGF-BB (R&D Systems, Inc., Minneapolis, MN, USA) group and PDGF-BB+GFK group. The concentration of PDGF-BB used for treatment was 10 ng/ml for 24 h at 37˚C, and the concentrations of GFK-medicated serum (Dalian Medical University) were 2, 4, 6, 8, 10, 12, 14 and 16%. Cell viability was measured using an MTT assay (Beyotime Institute of

Table I. Components of the herbal prescription Gan-fu-kang.

Herb name	Scientific name	Local name	Place of origin (China)	Relative quantity (g)
Salviae miltiorrhizae radix	*Salvia miltiorrhiza* Bunge	Dan Shen	Hebei	30
Milkvetch root	*Astragalus membranaceus* (Fisch.) Bunge	Huang Qi	Shanxi	30
Fructus aurantii	*Citrus aurantium* L.	ZhiKe	Hubei	20
Hoelen	*Poria cocos* (Schw.) Wolf	Fu Ling	Hubei	20
Radix paeoniae rubra	*Paeonia veitchii* Lynch	Chi Shao	Sichuan	15
Radix paeoniae alba	*Paeonia emodi* subsp. *sterniana* (H.R.Fletcher) Halda	Bai Shao	Anhui	15
Radix angelicae sinensis	*Angelica sinensis* (Oliv.) Diels	Dang Gui	Gansu	15
Radix rehmanniae	*Rehmannia chingii* H.L. Li	Di Huang	Liaoning	15
Rhizoma atractylodis macrocephalae	*Atractylodes macrocephala* Koidz.	Bai Zhu	Zhejiang	15
Radix bupleuri	*Bupleurum chinense* DC.	Chai Hu	Hubei	10
Radix glycyrrhizae	*Glycyrrhiza uralensis* Fisch.	Gan Cao	Neimenggu	10

Table II. Primer sequences and amplicon sizes.

Gene	Forward (5'-3')	Reverse (5'-3')	Product size (bp)
Wnt5a	AGGACTTACCTCGGGACTGG	TGCGACCTGCTTCATTGTT	171
Frizzled2	CCTGGAGGTGCATCAATTCTAC	CGCTCACCCAGAAACTTATAGC	447
CaMK II	TTCTACTGTTGCCTCCAT	AAAGTCCATCCCTTCCAC	460
Calcineurin	GGACAGGGTGGTGAAAGC	AGCGAGTGTTGGCAGGAG	296
NFAT	GCCCAGCGATGAGTATGAA	ATGCACCAGCACAGAACG	310
MMP-7	TGCCGGAGACTGGAAAGCTG	GGTGCAAAGGCATGGCCTAG	343
Collagen type I	TGCCGTGACCTCAAGATGTG	CACAAGCGTGCTGTAGGTGA	461
Collagen type III	AGATCATGTCTTGACTCAAGTC	TTTACATTGCCATTGGCCTGA	463
α-SMA	TGTGCTGGACTCTGGAGATG	GATCACCTGCCCATCAGG	291
β-actin	GGTATGGGTCAGAAGGACTCC	TGATCTTCAGGTGCTAGGAGCC	847

CaMK II, calmodulin-dependent kinase II; NFAT, nuclear factor of activated T cells; MMP,-7 matrix metalloproteinase-7; α-SMA, α-smooth muscle actin.

Biotechnology, Shanghai, China) at a wavelength of 490 nm, and cellular morphology was observed using phase-contrast microscopy (Olympus IX51; Olympus Corporation).

Immunohistochemistry. The liver tissue sections were deparaffinized using xylene (Nanjing Chemical Reagent Co., Ltd.), rehydrated with graded alcohols, treated with 0.3% endogenous peroxidase blocking solution (Sigma-Aldrich) for 20 min. Following high pressure heating retrieval (125˚C and 103 kPa) and non-immune goat serum (ZSGB-BIO, Beijing, China) blocking, the sections were incubated with one of the following primary antibodies purchased from BIOSS (Beijing, China): Rabbit anti-rat polyclonal anti-α-smooth muscle actin (SMA; 1:200; bs-0189R), anti-PDGF-BB (1:200; bs-1316R) and anti-PDGF receptor β (PDGFRβ; 1:150; bs-0232R). The primary antibodies were incubated overnight at 4˚C. Following washing with phosphate-buffered saline (PBS), goat anti-rabbit non-biotinylated regents (ZSGB-BIO; cat. no. PV-9001) were used to react with the primary antibody for 2 h at 37˚C, followed by the addition of diaminobenzidine (ZSGB-BIO) and monitoring of the staining. PBS was used as a negative control. In each section, five randomly-selected fields were examined using an Image-Pro Plus 6.0 analyzing system (Media Cybernetics, Inc., Rockville, MD, USA).

Western blotting. The manually homogenized liver tissues and cell lysates were treated with 150 µl radioimmunoprecipitation assay extraction buffer (Beyotime Institute of Biotechnology), and the supernatants were collected following centrifugation at 12,000 x g for 10 min at 4˚C. The concentration of total protein was estimated using a Bradford assay, with bovine serum albumin (BSA; Sigma-Aldrich) as a standard. The protein samples (10 µg) were subjected to 12% SDS-PAGE and were then transferred onto to polyvinylidene difluoride membranes

(EMD Millipore, Billerica, MA, USA). Following blocking with 5% BSA for 3 h at room temperature, the membranes were treated with the following primary antibodies: Rabbit anti-rat polyclonal antibodies against nuclear factor of activated T cells (NFAT; 1:200; Wuhan Boster Biological Technology, Ltd., Wuhan, China) and MMP7 (1:200; Wuhan Boster Biological Technology, Ltd.) overnight at 4˚C, washed with Tris-buffered saline containing 0.05% Tween 20 (TBST), and then incubated with peroxidase-conjugated secondary goat anti-rabbit antibody (1:2,000; Santa Cruz Biotechnology, Inc.; cat. no. sc-2004) for 2 h at room temperature. The membranes were washed with TBST and Prolight-horseradish peroxidase (Tiangen Biotech, Co., Ltd., Beijing, China) was used for blot detection. Rabbit anti-rat polyclonal β-actin antibodies (1:1,000; Santa Cruz Biotechnology, Inc.; cat. no. 130657) served as a loading control. Densitometric analysis was performed with LabWorks 4.6 (UVP, Inc., Upland, CA, USA).

Reverse transcription-polymerase chain reaction (RT-PCR) analysis. Total RNA was extracted from the liver tissues and cell lysates using TRIzol reagent, according to the manufacturer's protocol (Invitrogen; Thermo Fisher Scientific, Inc.). Reverse transcription with oligo (dT) primers (Tiangen Biotech, Co., Ltd.), Quant reverse transcriptase (Tiangen Biotech, Co., Ltd.) and dNTP mixture were used to synthesize complementary DNA (cDNA) from the total RNA. The primers were synthesized by Takara Biotechnology, Co., Ltd. (Dalian, China) for this purpose, and are as listed in Table II. A PCR reaction kit (Tiangen Biotech Co., Ltd.) containing 2 μl cDNA template, 12.5 μl 2X Taq PCR Master mix, 1 μl primers and 8.5 μl double distilled water to a total volume of 25 μl. Each sample had four replicates. The conditions for amplification were as follows: Wnt5a, Collagen type I, α-SMA, Calcineurin: One cycle of 94˚C for 5 min, 32 cycles of 94˚C for 30 sec, 64˚C for 30 sec, 72˚C for 30 sec, and a final extension of one cycle at 72˚C for 5 min; PDGF-BB and PDGFRβ: 30 cycles of 94˚C for 30 sec, 57˚C for 30 sec and 72˚C for 40 sec; Frizzled2: 35 cycles of 94˚C for 30 sec, 57˚C for 30 sec and 72˚C for 35 sec; NFAT: 32 cycles of 94˚C for 30 sec, 58˚C for 30 sec and 72˚C for 30 sec; calmodulin-dependent protein kinase II (CaMK II): 35 cycles of 94˚C for 30 sec, 56˚C for 30 sec and 72˚C for 40 sec; Collagen type III and β-actin: 32 cycles of 94˚C for 30 sec, 55˚C for 30 sec and 72˚C for 30 sec. The RT-PCR reaction was conducted using a T100 thermal cycler (Bio-Rad Laboratories, Inc., Hercules, CA, USA). The PCR products were electrophoresed on 2% agarose gels (Tiangen Biotech, Co., Ltd.) and the band density was measured using LabWorks 4.6. β-actin served as a loading control.

Statistical analysis. SPSS 19.0 statistical software (IBM SPSS, Armonk, NY, USA) was used for statistical analysis. All data are expressed as the mean ± standard deviation. Comparisons were performed using one-way analysis of variance. Ordinal data were analyzed using a Kruskal-Wallis test. P<0.05 was considered to indicate a statistically significant difference.

Results

GFK treatment reduces CCl_4-induced liver injury in rats. The degrees of hepatic damage in the rats were assessed by histopathological examination of the liver sections using H&E staining. As shown in Fig. 1A, compared with the control group, the livers of the CCl_4 treated rats exhibited marked fatty infiltration, bridging necrosis, damage of liver lobules and wide infiltration of inflammatory cells around the central vein. The livers of the rats in the GFK (31.25 mg/kg) group showed moderate widening and a fibrotic area with bridging fibrosis, which were also observed in the GFK (3,125 mg/kg) group. However, in the livers of the GFK (312.5 mg/kg)-treated rats, only mild focal fibrotic changes of the portal area and mild bridging were observed. The histopathological scores of liver fibrosis are shown in Table III.

Table III. Histopathological semi-quantitative scores of rat liver tissues.

Group	n	Hepatic fibrosis score (n)					Mean score
		0	1	2	3	4	
Control	12	12	0	0	0	0	5.5^b
CCl_4	8	0	0	2	3	3	44.82^a
CCl_4+GFK (3,125)	11	0	4	4	3	0	$33.17^{a,b}$
CCl_4+GFK (312.5)	11	0	7	4	0	0	$22.96^{a,b}$
CCl_4+GFK (31.25)	11	0	3	5	3	0	$31.85^{a,b}$

^{a}P<0.05, vs. control group; ^{b}P<0.05, vs. CCl_4 group. The concentrations of 3,125, 312.5 and 31.25 are in mg/kg. CCL_4, carbon tetrachloride; GFK, Gan-fu-kang.

CCl_4 treatment significantly increased the serum levels of AST and ALT by four and three-fold, respectively, and markedly decreased the serum levels of TP and ALB, compared with the control group (P<0.05). The administration of GFK markedly reduced the elevated levels in serum AST (P<0.05; 3,125 and 312.5 mg/kg) and ALT (P<0.05; 312.5 mg/kg), compared with the CCl_4 group. GFK treatment (312.5 mg/kg) significantly enhanced the CCl_4-induced decrease in the serum level of TP (P<0.05). The serum level of ALB showed a marginal increase in the GFK-treated groups (3,125 and 312.5 mg/kg), although without statistical significance (Fig. 1B).

GFK treatment attenuates CCl_4-induced collagen accumulation. Picro Sirius red staining was performed to observe collagen synthesis in the liver tissues. Collagen I was red and collagen III was green. Consistent with the H&E staining, the fibrotic changes were substantially decreased following administration of GFK at a dose of 312.5 mg/kg (Fig. 1A). Compared with the normal rats, CCl_4 administration caused a significant increase in the accumulation of collagen, as assessed by the hepatic Hyp content and mRNA expression levels of collagen type I and III. In the CCl_4-treated model group, the hepatic Hyp content was significantly increased, by three-fold, compared with the control group. GFK treatment notably reduced the elevated levels of Hyp, compared with the CCl_4 group, when treated at GFK concentrations of 312.5 and 3,125 mg/kg (P<0.05; Fig. 2A). The results of the RT-PCR analysis showed that treatment with various doses of GFK reduced the deposition of collagen type I and III in the CCl_4-induced fibrotic liver tissues (Fig. 2B).

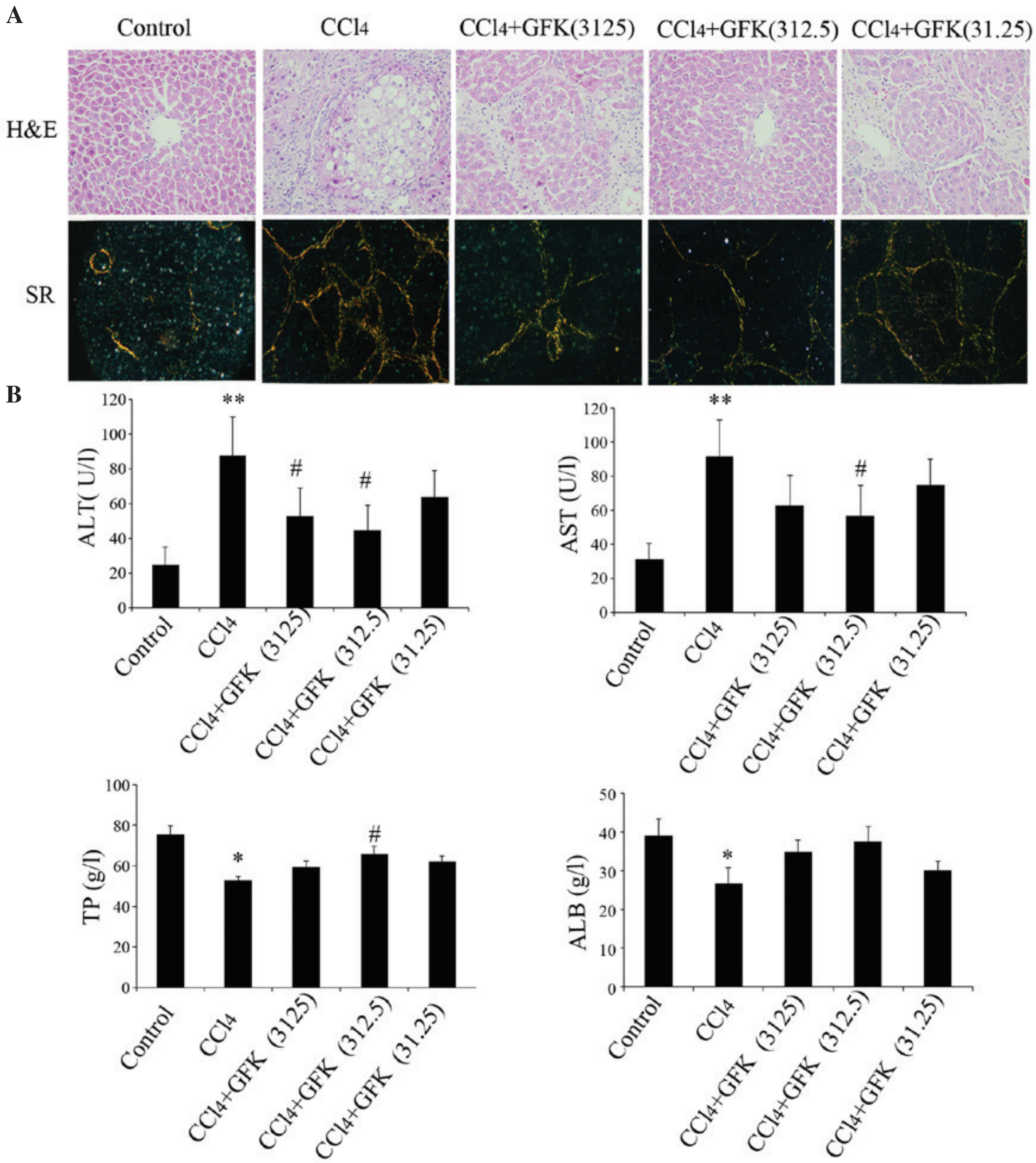

Figure 1. Effect of GFK on CCl_4-induced liver fibrosis. (A) GFK (312.5 mg/kg) attenuated pathological changes are shown by H&E (magnification, x400) and Sirius red staining (magnification, x200). (B) GFK reduced the levels of ALT and AST, and increased the level of TP at a dose of 312.5 mg/kg. Data are expressed as the mean ± standard deviation (n=10-12). *P<0.05 and **P<0.01, compared with the control group; $^{\#}$P<0.05, compared with the CCl_4 group. GFK, Gan-fu-kang; CCL_4, carbon tetrachloride; H&E, hematoxylin and eosin; SR, Sirius red; ALT, alanine aminotransferase; AST, aspartate aminotransferase; TP, total protein; ALB, albumin.

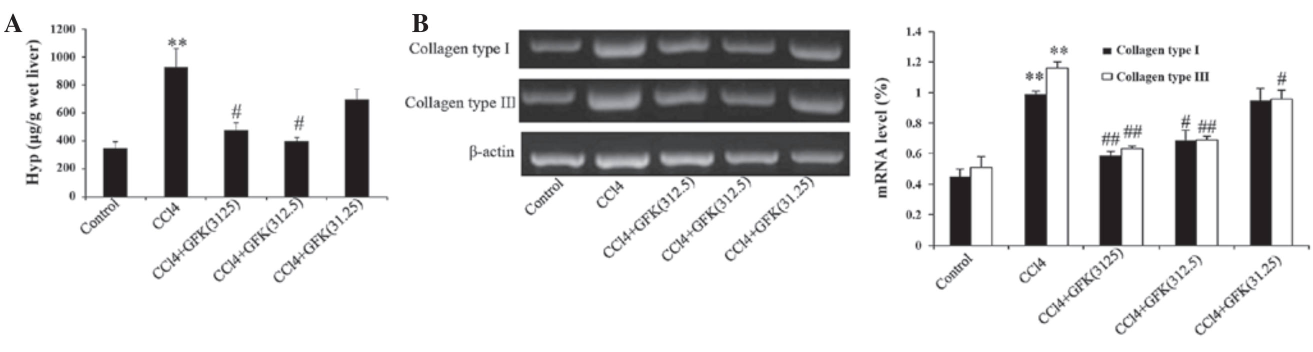

Figure 2. Effect of GFK on collagen accumulation. (A) Effect of GFK on the Hyp content of the liver tissues. Data are expressed as the mean ± standard deviation. **P<0.01, compared with the control group; $^{\#}$P<0.05, compared with the CCl_4 group. (B) Effects of GFK on the expression levels of collagen type I and collagen type III were determined using reverse transcription-quantitative polymerase chain reaction analysis. **P<0.01 vs. the control group and $^{\#}$P<0.05, $^{\#\#}$P<0.01 vs. the CCl_4 group. GFK, Gan-fu-kang; CCL_4, carbon tetrachloride; Hyp, hydroxyproline.

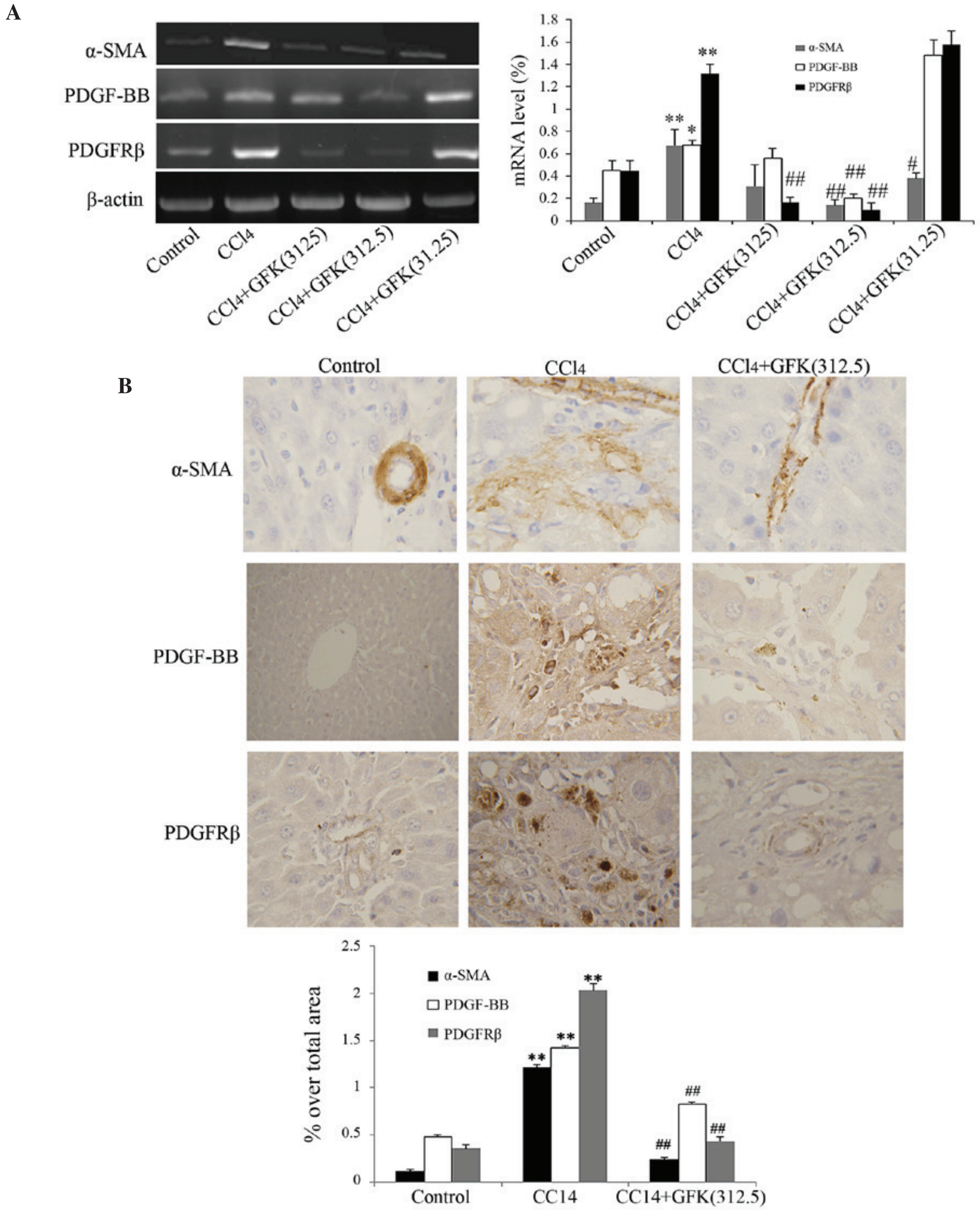

Figure 3. Effect of GFK on the activation of HSCs. (A) mRNA levels of α-SMA, PDGF-BB and PDGFRβ were significantly downregulated by GFK (312.5 mg/kg). Data are expressed as the mean ± standard deviation (n=5). (B) Immunohistochemical detection and evaluation of the expression levels of α-SMA, PDGF-BB and PDGFRβ in the rat liver tissues (magnification, x400). The areas of cells positive for α-SMA, PDGF-BB and PDGFRβ were reduced by GFK (312.5 mg/kg). *P<0.05 and **P<0.01, compared with the control group; #P<0.05 and ##P<0.01, compared with the CCl_4 groupGFK, Gan-fu-kang; CCL_4, carbon tetrachloride; PDGF, platelet-derived growth factor; α-SMA, α-smooth muscle actin; PDGFRβ, PDGF receptor β.

GFK treatment suppresses α-SMA activation, and the expression levels of PDGF-BB and PDGFRβ. α-SMA is a marker used to evaluate the degree of HSC activation (23). In addition, PDGF is one of the most potent mitogens for HSCs. Accordingly, PDGFRβ is expressed in HSCs when transformed, and may be a marker of HSC activation. In the present study, RT-PCR analysis revealed that the upregulation in the mRNA levels of α-SMA, PDGF-BB and PDGFRβ induced by CCl_4 were significantly attenuated by GFK (Fig. 3A). Image analysis of the immunohistochemical staining of α-SMA, PDGF-BB and PDGFRβ showed that, compared with the control group, CCl_4 treatment significantly increased the accumulation of activated HSCs (P<0.01; Fig. 3B). Treatment with the different doses of GFK significantly decreased HSC activation in the liver (P<0.01), with the medium dose (312.5 mg/kg) having the most pronounced effect on HSC activation (Fig. 3B).

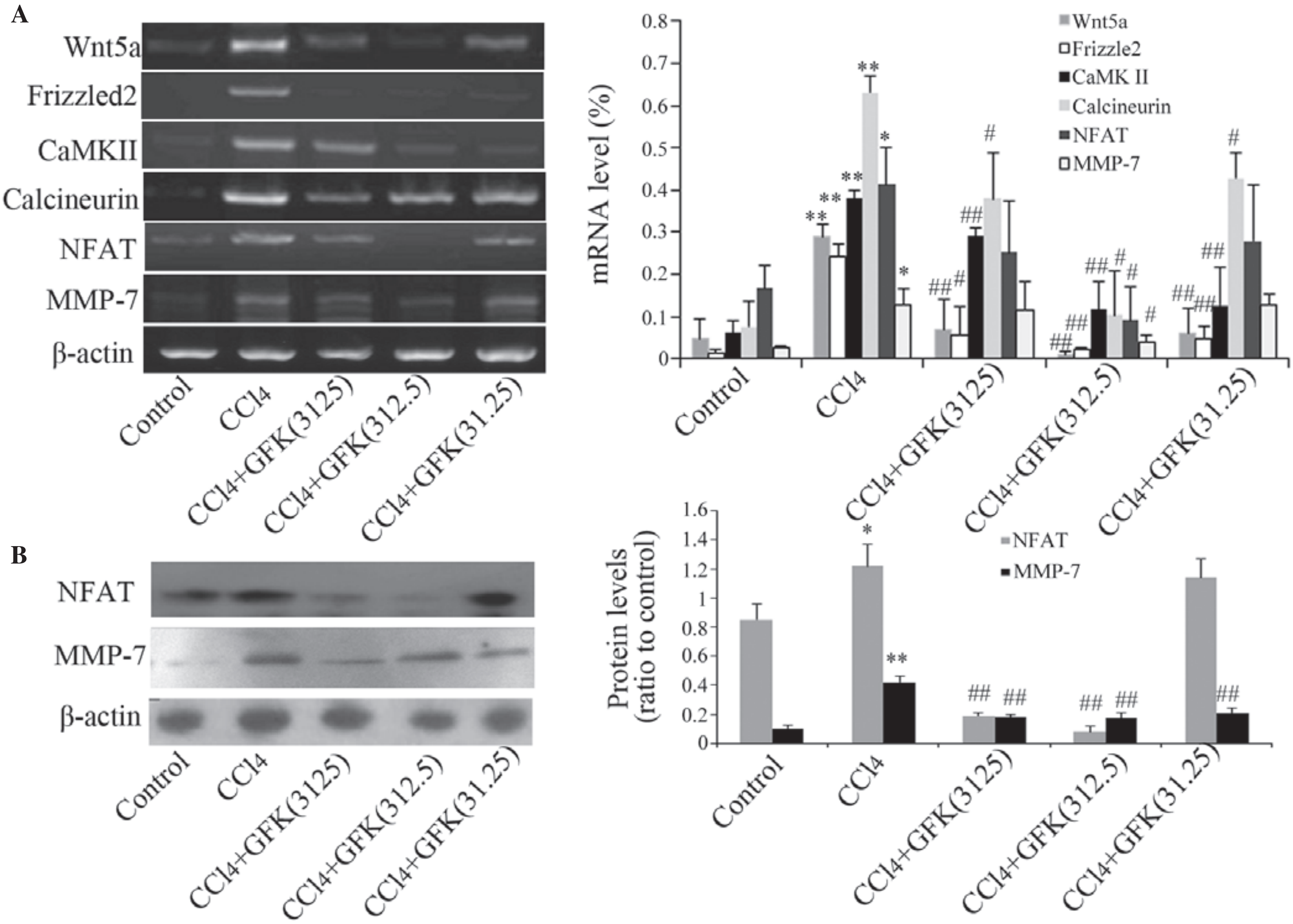

Figure 4. Effect of GFK on genes of the Wnt/Ca^{2+} signaling pathway. (A) Effect of GFK on the mRNA expression levels of genes in the Wnt/Ca^{2+} signaling pathway. (B) Effect of GFK on the expression levels of cytosolic NFAT and MMP-7, determined using Western blotting. CCl_4 treatment decreased the expression levels of NFAT and MMP-7, compared with those of the control group. Treatment with GFK at concentrations of 3,125 or 312.5 mg/kg increased the levels of NFAT and MMP-7. Data are expressed as the mean ± standard deviation (n=5). *P<0.05 and **P<0.01, compared with the control group; $^{\#}$P<0.05 and $^{\#\#}$P<0.01, compared wirh the CCl_4 group. GFK, Gan-fu-kang; CCL_4, carbon tetrachloride; NFAT, Nuclear factor of activated T cells; MMP-7, matrix metalloproteinase-7; CaMKII, calmodulin-dependent protein kinase II.

GFK treatment inhibits activation of the Wnt/Ca^{2+} signaling pathway in vivo. To elucidate the possible molecular pathway by which GFK suppressed liver fibrosis, the present study examined the mRNA and protein expression levels of several associated genes in the Wnt/Ca^{2+} signaling pathway. The mRNA expression levels of Wnt5a, Frizzled2, CaMK II, calcineurin, NFAT and MMP-7 were increased in the CCl_4-treated livers, compared with the control group. Following administration of GFK, the mRNA expression levels decreased at GFK dose of 312.5 mg/kg, compared with the CCl_4 group (Fig. 4A). Western blot analysis indicated a significant reduction in the protein levels of NFAT and MMP-7 (P<0.01; Fig. 4B). This suggested that GFK inhibits the Wnt/Ca^{2+} signaling pathway via protein synthesis levels rather than by repressing mRNA expression.

GFK treatment attenuates the proliferation and activation of HSC-T6 cells. To evaluate the effects of GFK on HSCs in the liver, HSC-T6 cells were treated with increasing concentrations of GFK. The MTT assay showed that GFK treatment caused a dose-dependent reduction in the number of HSC-T6 cells (Fig. 5A). The results revealed that GFK inhibited the viability, which was stimulated by PDGF-BB. The present study then calculated the half maximal inhibitory concentration (IC_{50}), which was used in the subsequent experiment. As shown in Fig. 5B, the HSCs cultured with PDGF-BB for 24 h exhibited an intermediate stage of the activation process. The HSCs exposed to GFK at the IC_{50} maintained a quiescent morphology. In addition, GFK treatment at the IC_{50} markedly decreased the expression levels of PDGFRβ, α-SMA, and collagen type I and III (Fig. 5C).

GFK treatment inhibits the Wnt/Ca^{2+} signaling pathway in HSC-T6 cells. The levels of principal elements in the Wnt/Ca^{2+} signaling pathway, including Wnt5a, Frizzled2, CaMK II, calcineurin, NFAT and MMP-7, were detected in HSC-T6 cells using RT-PCR and Western blot analyses. The results showed that the expression levels of these components were all attenuated in the presence of GFK at the IC_{50} (Fig. 6).

Discussion

At present, the major obstacles in the treatment of liver fibrosis are the unsatisfactory effects and various side effects due

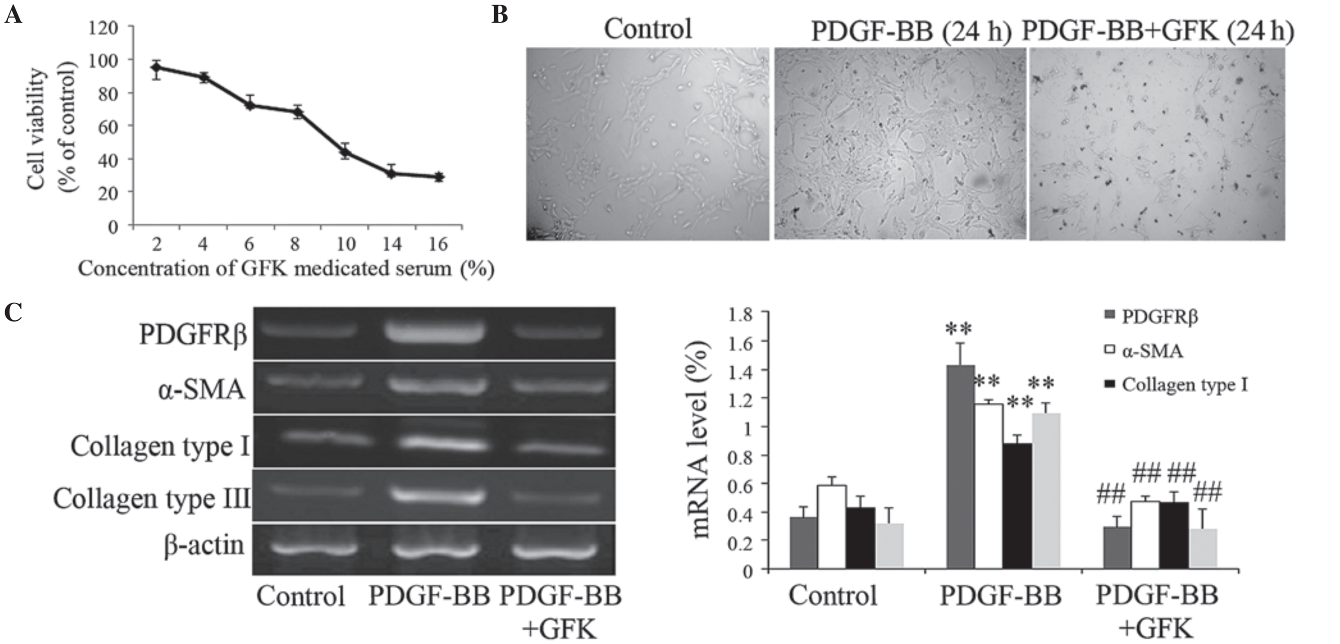

Figure 5. Effect of GFK on HSC-T6 cells. (A) Cell viability was detected using a 3-4,5-Dimethylthiazol-2-yl)-2,5-diphenyltetrazolium bromide assay. The results are expressed as the percentage of control cell viability at 24 h. (B) Effect of GFK treatment for 24 h on HSC-T6 cell morphology (magnification, x100). (C) Effect of GFK on the expression levels of PDGFRβ, α-SMA, and collagen type I and III in HSC-T6 cells. Data are expressed as the mean ± standard deviation (n=5). **P<0.01, compared with the control group; ##P<0.01, compared with the PDGF-BB treatment group. GFK, Gan-fu-kang; CCL4, carbon tetrachloride; α-SMA, α-smooth muscle actin; PDGF, platelet-derived growth factor; PDGFR, PDGF receptor β.

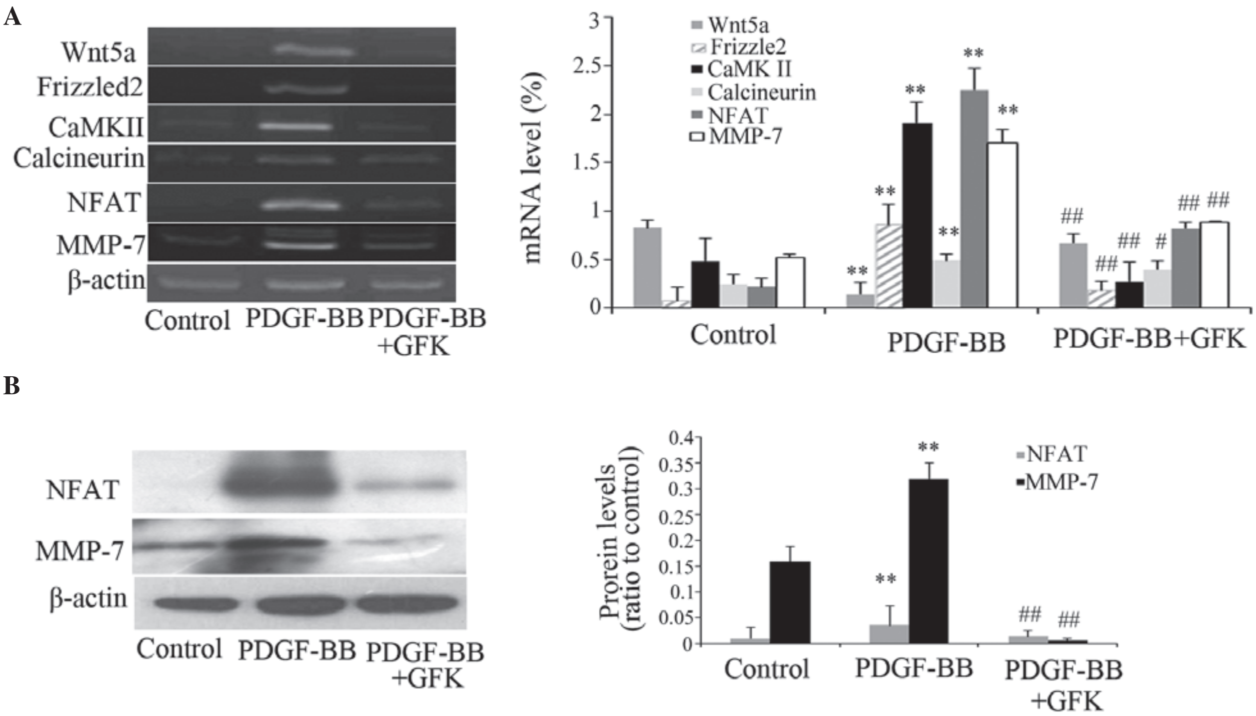

Figure 6. Effect of GFK on expression levels of Wnt/Ca^{2+} signaling pathway genes in HSC-T6 cells. (A) Reverse transcription-quantitative polymerase chain reaction analysis and quantification indicated activation of the Wnt/Ca^{2+} signaling pathway in the PDGF-BB-treated HSC-T6 cells. GFK significantly decreased the expression levels of these genes. (B) Western blot analysis was used to determine the expression levels of NFAT and MMP-7 in GFK-treated HSC-T6 cells. Data are expressed as the mean ± standard deviation (n=5). **P<0.01, compared with the control group; #P<0.05 and ##P<0.01, compared with the PDGF-BB treatment group. GFK, Gan-fu-kang; CCL4, carbon tetrachloride; PDGF, platelet-derived growth factor; PDGFR, PDGF receptor β; NFAT, Nuclear factor of activated T cells; MMP-7, matrix metalloproteinase-7; CaMKII, calmodulin-dependent protein kinase II.

to immune suppression and cytotoxicity (24). Medicinally, herbal drugs often provide alternative treatment options for liver diseases. GFK is a multi-ingredient herbal drug, which contains 11 crude plant ingredients. These 11 plants offer certain synergistic effects in hepatic injury therapy. One of the important components of GFK is *Astragalus membranaceus*, which has been found to significantly delay the formation of liver fibrosis induced by CCl_4 *in vivo* (25). The other major component in GFK, *Salvia miltiorrhiza*, can induce HSC apoptosis or inhibit the proliferation of HSCs (26). The remaining components of GFK, including Atractylodes macrocephala, Rehmannia glutinosa and licorice root, have been confirmed to have hepatoprotective effects (27-29). In the present study, the results showed that GFK suppresses the progress of CCl_4-induced liver fibrosis in rats. The data also indicated that GFK inhibited the proliferation of HSCs.

In the present study, as expected, histopathological examination (H&E staining) revealed that an 8-week period of subcutaneous injection of CCl_4 (0.5 mg/kg; twice per week) markedly induced hepatofibrotic changes, whereas GFK administration substantially ameliorate these alternations. These findings were also confirmed by the detection of the biochemical indicators, ALT, AST, TP and ALB. The progressive accumulation of ECM results in liver fibrosis. Collagen, particularly collagen type I and type III is the predominant component of the ECM, and Hyp is a degradation product of collagen, which has been used as an indicator for evaluating collagen deposition (30). The results of the present study showed that CCl_4 notably induced the accumulation of collagen, as determined by Hyp concentrations and Picric Sirius red staining, and that collagen deposition was markedly lowered by GFK treatment. It was also found that GFK administration significantly downregulated the expression levels of collagen type I and type III *in vivo* and *in vitro*, suggesting that GFK may enhance collagenolysis in the fibrotic liver.

It is generally accepted that HSCs are pivotal in the development of liver fibrosis, and that α-SMA is a key marker of HSC activation. In the present study, GFK was found to decrease HSC viability in a dose-dependent manner. Additionally, the data confirmed that GFK treatment (312.5 mg/kg) considerably inhibited the activation of HSCs, as observed in the immunohistochemical staining of α-SMA. The suppression of the gene expression levels of α-SMA in liver fibrosis and in the PDGF-BB-treated HSC-T6 cells were also more prominent in the GFK administration group. Consistent with the changes in levels of α-SMA, the expression levels of the profibrogenic cytokines, PDGF-BB and PDGFRβ, were marked in the fibrotic liver tissues, whereas they were attenuated following GFK treatment. In addition, GFK decreased the protein and mRNA levels of PDGF-BB and PDGFRβ *in vivo* and *in vitro*, demonstrating that the antifibrotic effects of GFK exerted its inhibitory effects on HSC activation via modulation of the profibrogenic cytokines, PDGF-BB and PDGFRβ.

The activation of Wnt signaling has been implicated in the conversion of numerous fibrotic diseases, including lung, heart, kidney and liver fibrosis (31-34). It has been demonstrated that the canonical and non-canonical Wnt signaling pathways are involved in the pathogenesis of liver fibrosis (35). The non-canonical Wnt/Ca^{2+} pathway includes the binding of Wnt5a to its receptor, Frizzled2, which then leads to elevated intracellular Ca^{2+} concentrations via a G-protein-dependent mechanism (36). Elevated Ca^{2+} can activate Ca^{2+}/CaMK II via calcineurin/NFAT pathways (37-39). The transcription factor, NFAT, translocates from the cytosol to the nucleus, thereby activating downstream target gene transcription (40). In the present study, the expression levels of components of the Wnt/Ca^{2+} signaling pathway, including Wnt5a, Frizzled2, CaMK II, calcineurin, NFAT and MMP-7, were markedly upregulated in the rats with hepatic fibrosis and the PDGF-BB-treated HSC-T6 cells. However, they were markedly decreased by GFK treatment. Furthermore, the effects on the protein levels of NFAT and MMP-7 were in accordance with the alterations in their mRNA expression levels. Taken together, these results suggested that GFK ameliorated liver fibrosis and activated HSCs by regulating the Wnt/Ca^{2+} signaling pathway.

Acknowledgements

This study was financially supported by the Natural Science Foundation of Liaoning Province, China (grant no. 201102055).

References

1. Friedman SL, Maher JJ and Bissell DM: Mechanisms and therapy of hepatic fibrosis: Report of the AASLD single topic basic research conference. Hepatology 32: 1403-1408, 2000.
2. Pellicoro A, Ramachandran P, Iredale JP and Fallowfield JA: Liver fibrosis and repair: Immune regulation of wound healing in a solid organ. Nat Rev Immunol 14: 181-194, 2014.
3. Puche JE, Saiman Y and Friedman SL: Hepatic stellate cells and liver fibrosis. Compr Physiol 3: 1473-1492, 2013.
4. Duval F, Moreno-Cuevas JE, González-Garza MT, Rodríguez-Montalvo C and Cruz-Vega DE: Liver fibrosis and protection mechanisms action of medicinal plants targeting apoptosis of hepatocytes and hepatic stellate cells. Adv Pharmacol Sci 2014: 373295, 2014.
5. Breitkopf K, Roeyen CV, Sawitza I, Wickert L, Floege J and Gressner AM: Expression patterns of PDGF-A, -B, -C and -D and the PDGF-receptors alpha and beta in activated rat hepatic stellate cells (HSC). Cytokine 31: 349-357, 2005.
6. Fang L, Zhan S, Huang C, Cheng X, Lv X, Si H and Li J: TRPM7 channel regulates PDGF-BB-induced proliferation of hepatic stellate cells via PI3 K and ERK pathways. Toxicol Appl Pharmacol 272: 713-725, 2013.
7. Shah R, Reyes-Gordillo K, Arellanes-Robledo J, Lechuga CG, Hernández-Nazara Z, Cotty A, Rojkind M and Lakshman MR: TGF-β 1 up-regulates the expression of PDGF-β receptor mRNA and induces a delayed PI3K-, AKT- and p70 S6K-dependent proliferative response in activated hepatic stellate cells. Alcohol Clin Exp Res 37: 1838-1848, 2013.
8. Miao CG, Yang YY, He X, Huang C, Huang Y, Zhang L, Lv XW, Jin Y and Li J: Wnt signaling in liver fibrosis: Progress, challenges and potential directions. Biochimie 95: 2326-2335, 2013.
9. Al-Harthi L: Wnt/β-catenin and its diverse physiological cell signaling pathways in neurodegenerative and neuropsychiatric disorders. J Neuroimmune Pharmacol 7: 725-730, 2012.
10. Holland JD, Klaus A, Garratt AN and Birchmeier W: Wnt signaling in stem and cancer stem cells. Curr Opin Cell Biol 25: 254-264, 2013.
11. Ge WS, Wang YJ, Wu JX, Fan JG, Chen YW and Zhu L: β-catenin is overexpressed in hepatic fibrosis and blockage of Wnt/β-catenin signaling inhibits hepatic stellate cell activation. Mol Med Rep 9: 2145-2151, 2014.
12. Rashid ST, Humphries JD, Byron A, Dhar A, Askari JA, Selley JN, Knight D, Goldin RD, Thursz M and Humphries MJ: Proteomic analysis of extracellular matrix from the hepatic stellate cell line LX-2 identifies CYR61 and Wnt-5a as novel constituents of fibrotic liver. J Proteome Res 11: 4052-4064, 2012.
13. MadanKumar P, NaveenKumar P, Manikandan S, Devaraj H and NiranjaliDevaraj S: Morin ameliorates chemically induced liver fibrosis in vivo and inhibits stellate cell proliferation in vitro by suppressing Wnt/β-catenin signaling. Toxicol Appl Pharmacol 277: 210-220, 2014.
14. Shin HW, Park SY, Lee KB, Shin E, Nam SW, Lee JY and Jang JJ: Transcriptional profiling and Wnt signaling activation in proliferation of human hepatic stellate cells induced by PDGF-BB. Korean J Hepatol 15: 486-495, 2009.

15. Saneyoshi T, Kume S, Amasaki Y and Mikoshiba K: The Wnt/calcium pathway activates NF-AT and promotes ventral cell fate in Xenopus embryos. Nature 417: 295-299, 2002.
16. Wei F, Lang Y, Gong D and Fan Y: Effect of Dahuang zhechong formula on liver fibrosis in patients with chronic hepatitis B: A meta-analysis. Complement Ther Med 23: 129-138, 2015.
17. Lin HJ, Chen JY, Lin CF, Kao ST, Cheng JC, Chen HL and Chen CM: Hepatoprotective effects of Yi Guan Jian, an herbal medicine, in rats with dimethylnitrosamine-induced liver fibrosis. J Ethnopharmacol 134: 953-960, 2011.
18. Xu TT, Jiang MN, Li C, Che Y and Jia YJ: Effect of Chinese traditional compound, Gan-fu-kang, on CCl(4)-induced liver fibrosis in rats and its probable molecular mechanisms. Hepatol Res 37: 221-229, 2007.
19. Lou JL, Jiang MN, Li C, Zhou Q, He X, Lei HY, Li J and Jia YJ: Herb medicine Gan-fu-kang attenuates liver injury in a rat fibrotic model. J Ethnopharmacol 128: 131-138, 2010.
20. Zhang C, Wang Y, Chen H, Yang G, Wang S, Jiang M, Cong L, Yuan L, Li H and Jia Y: Protective effect of the herbal medicine Gan-fu-kang against carbon tetrachloride-induced liver fibrosis in rats. Mol Med Rep 8: 954-962, 2013.
21. National Institutes of Health: Guide for the Care and Use of Laboratory Animals. 6th edition. National Academies Press, Washington, DC, 1985.
22. Scheuer PJ: Classification of chronic viral hepatitis: A need for reassessment. J Hepatol 13: 372-374, 1991.
23. Zakaria S, Youssef M, Moussa M, Akl M, El-Ahwany E, El-Raziky M, Mostafa O, Helmy AH and El-Hindawi A: Value of α-smooth muscle actin and glial fibrillary acidic protein in predicting early hepatic fibrosis in chronic hepatitis C virus infection. Arch Med Sci 6 : 356-365, 2010.
24. Schiavon F: Transient joint effusion: A forgotten side effect of high dose corticosteroid treatment. Ann Rheum Dis 62: 491-492, 2003.
25. Sun WY, Wang L, Liu H, Li X and Wei W: A standardized extract from *Paeonia lactiflora* and *Astragalus membranaceus* attenuates liver fibrosis induced by porcine serum in rats. Int J Mol Med 29: 491-498, 2012.
26. Lee HS, Son WC, Ryu JE, Koo BA and Kim YS: Standardized *Salvia miltiorrhiza* extract suppresses hepatic stellate cell activation and attenuates steatohepatitis induced by a methionine-choline deficient diet in mice. Molecules 19: 8189-8211, 2014.
27. Jin C, Zhang PJ, Bao CQ, Gu YL, Xu BH, Li CW, Li JP, Bo P and Liu XN: Protective effects of Atractylodes macrocephala polysaccharide on liver ischemia-reperfusion injury and its possible mechanism in rats. Am J Chin Med 39: 489-502, 2011.
28. Wu PS, Wu SJ, Tsai YH, Lin YH and Chao JC: Hot water extracted Lycium barbarum and Rehmannia glutinosa inhibit liver inflammation and fibrosis in rats. Am J Chin Med 39: 1173-1191, 2011.
29. Hajiaghamohammadi AA, Ziaee A and Samimi R: The efficacy of licorice root extract in decreasing transaminase activities in non-alcoholic fatty liver disease: A randomized controlled clinical trial. Phytother Res 26: 1381-1384, 2012.
30. Hofman K, Hall B, Cleaver H and Marshall S: High-throughput quantification of hydroxyproline for determination of collagen. Anal Biochem 417: 289-291, 2011.
31. Song P, Zheng JX, Xu J, Liu JZ, Wu LY and Liu C: β-catenin induces A549 alveolar epithelial cell mesenchymal transition during pulmonary fibrosis. Mol Med Rep 11: 2703-2710, 2015.
32. Ye B, Ge Y, Perens G, Hong L, Xu H, Fishbein MC and Li F: Canonical Wnt/β-catenin signaling in epicardial fibrosis of failed pediatric heart allografts with diastolic dysfunction. Cardiovasc Pathol 22: 54-57, 2013.
33. Li X, Yamagata K, Nishita M, Endo M, Arfian N, Rikitake Y, Emoto N, Hirata K, Tanaka Y and Minami Y: Activation of Wnt5a-Ror2 signaling associated with epithelial-to-mesenchymal transition of tubular epithelial cells during renal fibrosis. Genes Cells 18: 608-619, 2013.
34. Li W, Zhu C, Li Y, Wu Q and Gao R: Mest attenuates CCl4-induced liver fibrosis in rats by inhibiting the Wnt/β-catenin signaling pathway. Gut Liver 8: 282-291, 2014.
35. Jiang F, Parsons CJ and Stefanovic B: Gene expression profile of quiescent and activated rat hepatic stellate-cells implicates Wnt signaling pathway in activation. J Hepatol 45: 401-409, 2006.
36. Sheldahl LC, Park M, Malbon CC and Moon RT: Protein kinase C is differentially stimulated by Wnt and Frizzled homologs in a G-protein-dependent manner. Curr Biol 9: 695-698, 1999.
37. De A: Wnt/Ca^{2+} signaling pathway: A brief overview. Acta Biochim Biophys Sin (Shanghai) 43: 745-756, 2011.
38. Buchholz M, Schatz A, Wagner M, Michl P, Linhart T, Adler G, Gress TM and Ellenrieder V: Overexpression of c-myc in pancreatic cancer caused by ectopic activation of NFATc1 and the Ca^{2+}/calcineurin signaling pathway. EMBO J 25: 3714-3724, 2006.
39. Kohn AD and Moon RT: Wnt and calcium signaling: Beta-catenin-independent pathways. Cell Calcium 38: 439-446, 2005.
40. Kim J, Kim DW, Chang W, Choe J, Kim J, Park CS, Song K and Lee I: Wnt5a is secreted by follicular dendritic cells to protect germinal center B cells via Wnt/Ca^{2+}/NFAT/NF-κB-B cell lymphoma 6 signaling. J Immunol 188: 182-189, 2012.